Fast Passivity Assessment for S-Parameter Rational Models Via a Half-Size Test Matrix

Bjørn Gustavsen, *Senior Member, IEEE*, and Adam Semlyen, *Life Fellow, IEEE*

***Abstract*—Rational models must be passive in order to ensure stable time domain simulations. The assessment of passivity properties is usually done via a Hamiltonian matrix that is associated with the state-space model, allowing precise characterization of passivity violations from its imaginary eigenvalues. The calculation of eigenvalues can be time consuming for large models as the matrix size is equal to twice the number of model states. In this paper, we derive for S-parameter models a new test matrix which is only half the size of the Hamiltonian matrix. This leads to savings in the eigenvalue computation time by a factor of nearly eight. The new test matrix takes into account that the model is symmetrical, in pole-residue form. Its application is demonstrated by three examples: a microwave filter, a package, and a synthetic model.**

***Index Terms*—Hamiltonian matrix, macromodel, passivity, passivity assessment, rational model, S-parameters.**

I. Introduction

TIME-DOMAIN simulation plays a crucial role in the design and verification of high-speed electronic circuits and communication systems. The modeling of the system parts is becoming more challenging as the bit rates keep increasing, giving rise to higher levels of undesired phenomena such as pulse distortion, wave reflection, and crosstalk.

Rational modeling is a convenient way of representing linear parts of the system with inclusion of frequency-dependent effects. The modeling starts from a set of port responses that characterize the behavior of the model. The parameters may come from electromagnetic computations in the frequency domain or the time domain or from frequency-domain measurements. The parameters can be in the form of admittance parameters, but more often scattering (S-) parameters are used. The rational modeling can be easily performed in the frequency domain using the pole-relocating method known as vector fitting [1]–[4] which has also been adopted for the time domain [5] and the z-domain [6].

Although the model obtained via vector fitting has guaranteed stable poles, the model may result in unstable simulations because the passivity of the model is not assured. Several methods have been proposed which aim at enforcing passivity by a perturbation of the model parameters. All of these methods require the ability to assess the passivity characteristics of the model. For that purpose, it is common practice to calculate the eigenvalues of a Hamiltonian matrix which is associated with a state-space formulation of the model [7]–[9]. The imaginary eigenvalues define frequency boundaries for passivity violations, thereby allowing to pinpoint frequency intervals where the model is nonpassive.

A difficulty with the Hamiltonian matrix is its size. Its dimension is two times the number of system states, which makes the computation of eigenvalues time-consuming for large models. It has been proposed [10], [11] to reduce the computation time by calculating only the (few) imaginary eigenvalues, but a reliable implementation is not easy. In [12], a half-size test matrix was derived for use with models based on admittance (Y-) parameters. The use of a half-size matrix reduces the eigenvalue computation time by a factor of nearly eight due to the cubic complexity of eigenvalue computation.

In this paper, we derive a half-size test matrix for use with models based on scattering (S-) parameters. This is motivated by the fact that the eigenvalues appear in pairs and quadruples, thus representing redundant information. First, we show that a symmetrical pole-residue model implies a symmetrical state-space model. Using this information, we subject the Hamiltonian matrix to a similarity transformation, which reduces the original eigenvalue problem to a half-size problem. The square roots of the eigenvalues of the new test matrix are equal to the eigenvalues of the Hamiltonian matrix, without redundancy. In the actual implementation, we first convert the state-space model into a real-only model, giving even faster computations and noiseless eigenvalues. The new test matrix is applied to the models of a microwave filter and of a package, demonstrating the validity of the approach and the speed advantage over the Hamiltonian matrix. A small synthetic example is included so that the reader can verify the procedure. We also show a simple derivation of the Hamiltonian matrix using state equations, and we prove that the conversion of the state-space model into a real-only model does not alter the eigenvalues of the new test matrix. All computations are with Matlab running on a desktop computer with a 1.3-GHz Pentium processor.

II. Rational Modeling

In this study, we will assume a symmetrical scattering matrix $\boldsymbol{S}$. The symmetry results for reciprocal n-port elements with proper normalization of the port reference impedances. A convenient way of calculating a rational approximation is to subject

Manuscript received April 04, 2008; revised July 30, 2008. First published November 18, 2008; current version published December 05, 2008. The work of B. Gustavsen was supported in part by the Norwegian Research Council, Compagnie Deutsch, FMC Technologies, Framo, Norsk Hydro, Petrobras, Prysmian, Siemens, Statoil, Total, and Vetco Gray.

B. Gustavsen is with SINTEF Energy Research, N-7465 Trondheim, Norway (e-mail: bjorn.gustavsen@sintef.no).

A. Semlyen is with the Department of Electrical and Computer Engineering, University of Toronto, Toronto, ON, Canada M5S 3G4 (e-mail: adam.semlyen@utoronto.ca).

Color versions of one or more of the figures in this paper are available online at http://ieeexplore.ieee.org.

Digital Object Identifier 10.1109/TMTT.2008.2007319

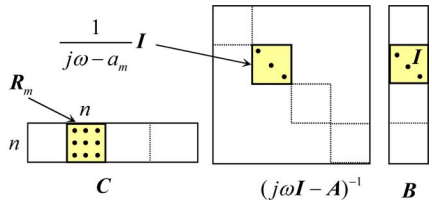

Fig. 1. Contribution from the mth term in (1) to the state-space model (2).

the upper triangle part of $\boldsymbol{S}$ to fitting by vector fitting. This leads to a pole-residue model equation

$$\boldsymbol{S}(\omega) = \sum_{m=1}^{N} \frac{\boldsymbol{R}_m}{j\omega - a_m} + \boldsymbol{D} \tag{1}$$

with symmetrical residue matrices and guaranteed stable poles. The poles $\{a_m\}$ and residue matrices $\{\boldsymbol{R}_m\}$ are either real or come in complex conjugate pairs. The constant term $\boldsymbol{D}$ is real and symmetrical. For an n-port model, $\boldsymbol{S}$, $\{\boldsymbol{R}_m\}$ and $\boldsymbol{D}$ are of dimension $n \times n$.

For the purpose of passivity assessment, the pole-residue model must first be cast in the form of a state-space model

$$\boldsymbol{S}(\omega) = \boldsymbol{C}(j\omega\boldsymbol{I} - \boldsymbol{A})^{-1}\boldsymbol{B} + \boldsymbol{D}. \tag{2}$$

Each pole-residue term in (1) is factorized; see

$$\frac{\boldsymbol{R}_m}{j\omega - a_m} = \boldsymbol{R}_m \left(\frac{1}{j\omega - a_m} \boldsymbol{I} \right) \boldsymbol{I} \tag{3}$$

where $\boldsymbol{I}$ is the identity matrix of the same dimension as $\boldsymbol{R}_m$ [13].

This shows that the mth pole-residue term gives a state-space model with $\boldsymbol{C}_m$ equal to $\boldsymbol{R}_m$, $\boldsymbol{A}_m$ diagonal with a_m repeated n times, and $\boldsymbol{B}_m$ equal to $\boldsymbol{I}$. The N state-space models are concatenated into a single state-space model

$$\begin{aligned} \boldsymbol{C} &= [\boldsymbol{R} \quad \ldots \quad \boldsymbol{R}_N] \\ \boldsymbol{A} &= \mathrm{diag}(\boldsymbol{A}_1 \quad \ldots \quad \boldsymbol{A}_N) \\ \boldsymbol{B} &= [\boldsymbol{I} \quad \ldots \quad \boldsymbol{I}]^T. \end{aligned} \tag{4}$$

The building of $\boldsymbol{A}$, $\boldsymbol{B}$, and $\boldsymbol{C}$ from (1) via (3) is illustrated in Fig. 1, with $n = 3$ and $N = 4$.

Finally, we rearrange the columns in $\boldsymbol{C}$, rows in $\boldsymbol{B}$, and rows and columns of $\boldsymbol{A}$ to produce a column-wise realization; see Appendix A. This rearrangement causes the complex pairs to appear in consecutive pairs on the diagonal of $\boldsymbol{A}$.

III. Passivity Assessment Via Hamiltonian Matrix

The passivity of the model entails that the model cannot generate energy, at whatever terminal conditions. In the case of scattering parameters, the transfer matrix $\boldsymbol{S}$ must be bounded by unity, i.e.,

$$(\boldsymbol{I} - \boldsymbol{S}(\omega)^H \boldsymbol{S}(\omega)) > 0. \tag{5}$$

This implies that all singular values σ of $\boldsymbol{S}$ are smaller than unity, at all frequencies,

$$\sigma_i(\omega) < 1, \qquad i = 1...n. \tag{6}$$

The singular values are given by the singular value decomposition

$$\boldsymbol{S}(\omega) = \boldsymbol{U}(\omega)\boldsymbol{\Sigma}(\omega)\boldsymbol{V}^H(\omega) \tag{7}$$

where $\boldsymbol{\Sigma}$ is a diagonal matrix containing the singular values.

A precise way of assessing the passivity properties of a state-space model is to calculate the eigenvalues of the Hamiltonian matrix $\boldsymbol{M}$ [9] as

$$\boldsymbol{M} = \begin{bmatrix} \boldsymbol{A} - \boldsymbol{B}\hat{\boldsymbol{R}}^{-1}\boldsymbol{D}^T\boldsymbol{C} & -\boldsymbol{B}\hat{\boldsymbol{R}}^{-1}\boldsymbol{B}^T \\ \boldsymbol{C}^T\hat{\boldsymbol{S}}^{-1}\boldsymbol{C} & -\boldsymbol{A}^T + \boldsymbol{C}^T\boldsymbol{D}\hat{\boldsymbol{R}}^{-1}\boldsymbol{B}^T \end{bmatrix} \tag{8}$$

where $\hat{\boldsymbol{R}} = (\boldsymbol{D}^T\boldsymbol{D} - \boldsymbol{I})$ and $\hat{\boldsymbol{S}} = (\boldsymbol{D}\boldsymbol{D}^T - \boldsymbol{I})$.

The model is passive if its Hamiltonian matrix has no purely imaginary eigenvalues and any imaginary eigenvalue defines a crossover frequency where a singular value changes from being smaller than unity to larger than unity, or vice versa.

This approach is widely applied [9], offering a much more reliable approach than sweeping the singular values over a grid of discrete frequencies.

Appendix B shows a simple derivation of $\boldsymbol{M}$ in (8) using only state equations, which makes it easy to understand by a wide segment of readers.

IV. Symmetrical State-Space Model

In what follows, we show that a symmetrical pole-residue model implies a state-space model with $\boldsymbol{C} = \boldsymbol{B}^T$. This result is essential for the derivations in Section V.

Each residue matrix $\{\boldsymbol{R}_m\}$ is subjected to the eigenvalue decomposition

$$\boldsymbol{R} = \boldsymbol{T}\boldsymbol{\Lambda}\boldsymbol{T}^{-1} = \boldsymbol{T}\boldsymbol{Q} = \sum_{i=1}^{n} \boldsymbol{t}_i \boldsymbol{q}_i^T \tag{9}$$

where $\boldsymbol{\Lambda}$ is a diagonal matrix containing the eigenvalues. The eigenvalue matrix $\boldsymbol{\Lambda}$ is multiplied with the inverse eigenvector matrix $\boldsymbol{T}^{-1}$ to form a scaled matrix $\boldsymbol{Q}$, and the resulting matrix product $\boldsymbol{T}\boldsymbol{Q}$ is expanded into a sum of outer products.

The columns $\boldsymbol{t}_i$ and rows $\boldsymbol{q}_i^T$ are rescaled using the diagonal elements of $\boldsymbol{T}$ and $\boldsymbol{Q}$, which makes them equal

$$\tilde{\boldsymbol{t}}_i = \sqrt{\frac{\boldsymbol{Q}_{ii}}{\boldsymbol{T}_{ii}}}\boldsymbol{t}_i, \quad \tilde{\boldsymbol{q}}_i = \sqrt{\frac{\boldsymbol{T}_{ii}}{\boldsymbol{Q}_{ii}}}\boldsymbol{q}_i. \tag{10}$$

The symmetrical state-space model associated with each pole-residue term is formed as shown in

$$\boldsymbol{C} = [\tilde{\boldsymbol{t}}_1 \quad \ldots \quad \tilde{\boldsymbol{t}}_n] \quad \boldsymbol{A} = \mathrm{diag}(a \quad \ldots \quad a) \quad \boldsymbol{B} = \boldsymbol{C}^T. \tag{11}$$

The columns $\tilde{\boldsymbol{t}}_i$ are introduced as columns in $\boldsymbol{C}$ and rows in $\boldsymbol{B}$, and the poles a are repeated n times on the diagonal. Finally, the state-space models from all pole-residue terms are concatenated into a single model (11).

Since $\tilde{\boldsymbol{t}}_i$ was used in both $\boldsymbol{C}$ (columns) and $\boldsymbol{B}$ (rows), it follows that $\boldsymbol{C} = \boldsymbol{B}^T$.

V. Half-Size Passivity Test Matrix

For the symmetrical state-space model (with $\boldsymbol{C} = \boldsymbol{B}^T$, $\boldsymbol{D} = \boldsymbol{D}^T$) we get for the Hamiltonian matrix (8)

$$\boldsymbol{M} = \begin{bmatrix} \boldsymbol{E} & \boldsymbol{F} \\ -\boldsymbol{F} & -\boldsymbol{E} \end{bmatrix} \tag{12a}$$

where

$$\boldsymbol{E} = \boldsymbol{A} - \boldsymbol{B}(\boldsymbol{D}^2 - \boldsymbol{I})^{-1}\boldsymbol{D}^T\boldsymbol{C} \tag{12b}$$

$$\boldsymbol{F} = -\boldsymbol{B}(\boldsymbol{D}^2 - \boldsymbol{I})^{-1}\boldsymbol{C}. \tag{12c}$$

Introducing the similarity transformation

$$\tilde{\boldsymbol{M}} = \boldsymbol{T}^{-1}\boldsymbol{M}\boldsymbol{T} \tag{13a}$$

$$\boldsymbol{T} = \begin{bmatrix} \boldsymbol{I} & \boldsymbol{I} \\ \boldsymbol{I} & -\boldsymbol{I} \end{bmatrix}$$

$$\boldsymbol{T}^{-1} = \frac{1}{2}\boldsymbol{T} \tag{13b}$$

gives the transformed Hamiltonian $\tilde{\boldsymbol{M}}$

$$\tilde{\boldsymbol{M}} = \begin{bmatrix} 0 & \boldsymbol{E} - \boldsymbol{F} \\ \boldsymbol{E} + \boldsymbol{F} & 0 \end{bmatrix}. \tag{14}$$

Each pair of eigenvalue λ and eigenvector $\boldsymbol{x}$ of $\tilde{\boldsymbol{M}}$ is given by

$$(\tilde{\boldsymbol{M}} - \lambda \boldsymbol{I}_d)\boldsymbol{x} = 0 \tag{15a}$$

$$\begin{bmatrix} -\lambda\boldsymbol{I} & (\boldsymbol{E} - \boldsymbol{F}) \\ (\boldsymbol{E} + \boldsymbol{F}) & -\lambda\boldsymbol{I} \end{bmatrix} \begin{bmatrix} \boldsymbol{x}_1 \\ \boldsymbol{x}_2 \end{bmatrix} = \begin{bmatrix} 0 \\ 0 \end{bmatrix}. \tag{15b}$$

Solving the first equation of (15b) for $\boldsymbol{x}_1$ and substituting into the second equation gives

$$[(\boldsymbol{E} + \boldsymbol{F})(\boldsymbol{E} - \boldsymbol{F}) - \lambda^2\boldsymbol{I}]\boldsymbol{x}_2 = 0. \tag{16}$$

From this, it follows that the eigenvalues of $\tilde{\boldsymbol{M}}$ (and thus of $\boldsymbol{M}$) can be calculated as the square-roots of the eigenvalues of the half-size matrix

$$\boldsymbol{P} = (\boldsymbol{E} + \boldsymbol{F})(\boldsymbol{E} - \boldsymbol{F}) \tag{17}$$

which, after inserting (12b) for $\boldsymbol{E}$ and (12c) for $\boldsymbol{F}$, becomes

$$\boldsymbol{P} = (\boldsymbol{A} - \boldsymbol{B}(\boldsymbol{D} - \boldsymbol{I})^{-1}\boldsymbol{C})(\boldsymbol{A} - \boldsymbol{B}(\boldsymbol{D} + \boldsymbol{I})^{-1}\boldsymbol{C}). \tag{18}$$

Thus

$$\lambda_{\boldsymbol{M}} = \pm\sqrt{\lambda_{\boldsymbol{P}}}. \tag{19}$$

We denote the matrix $\boldsymbol{P}$ a "passivity matrix." It is not a Hamiltonian matrix.

Theorem: The passivity matrix $\boldsymbol{P}$ gives, via the subset of its negative-real eigenvalues $-\omega^2$, the frequencies $j\omega$, which are the boundaries of passivity violations.

Note that the conversion of the state-space model into a symmetrical state-space model as described in Section IV does not need to be carried out. This conversion only served to facilitate the derivation of $\boldsymbol{P}$ when moving from (12) to (14). Thus, the calculation of $\boldsymbol{P}$ can be done by (18) even when we do not have $\boldsymbol{C} = \boldsymbol{B}^T$, as the properties of the state-space model are not affected by the conversion. The only requirement is that the state-space model represent a symmetrical $\boldsymbol{S}$, which is always the case when starting with a pole-residue model with symmetrical residue matrices $\{\boldsymbol{R}_m\}$ and a symmetrical $\boldsymbol{D}$.

VI. Conversion Into Real-Only State-Space Model

It is preferable to convert the complex $\boldsymbol{P}$ into a real-only matrix before computing its eigenvalues. This has the advantage of faster eigenvalue computation. In Matlab, a speedup by a factor of about four is achieved.

For each pair, the corresponding submatrices of the columnwise state-space realization (Appendix A) are modified (via a similarity transformation) into a real-only model as follows [14]:

$$\hat{\mathbf{A}} = \begin{bmatrix} \mathrm{Re}\{a\} & \mathrm{Im}\{a\} \\ -\mathrm{Im}\{a\} & \mathrm{Re}\{a\} \end{bmatrix}$$

$$\hat{\mathbf{c}} = [\,\mathrm{Re}\{\mathbf{c}\} \quad \mathrm{Im}\{\mathbf{c}\}\,] \tag{20a}$$

$$\hat{\mathbf{b}} = \begin{bmatrix} 2\mathrm{Re}\{\mathbf{b}^T\} \\ -2\mathrm{Im}\{\mathbf{b}^T\} \end{bmatrix} = \begin{bmatrix} 2\mathrm{Re}\{\mathbf{b}^T\} \\ 0 \end{bmatrix}. \tag{20b}$$

In Appendix C, we prove that the conversion equation (20) will not change the eigenvalues of $\boldsymbol{P}$.

VII. Example: Microwave Filter

This example considers a rational model of a two-port hairpin microwave filter [15]. The model has ten pole-residue terms and a nonzero $\boldsymbol{D}$. The frequency response $\boldsymbol{S}(\omega)$ is shown in Fig. 2.

The pole-residue model is converted into a real-only state-space model by the similarity transformation (20). Table I compares the imaginary eigenvalues of the state-space model when calculated using either the Hamiltonian matrix $\boldsymbol{M}$ [(8)] or the half-size passivity matrix $\boldsymbol{P}$ [(18)]. It is observed that the usage of $\boldsymbol{P}$ leads to exactly the same eigenvalues as $\boldsymbol{M}$ but without redundant information. It is also observed that the real parts in

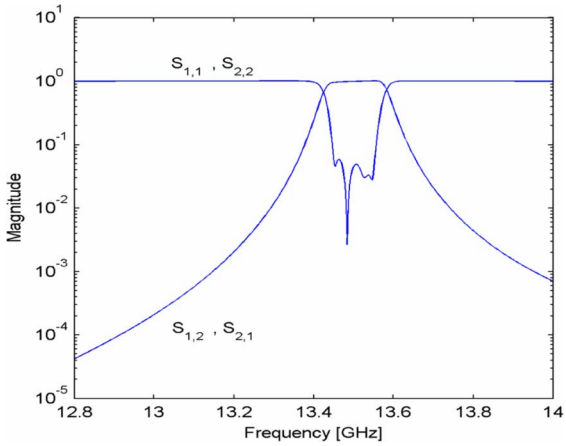

Fig. 2. Rational model: elements of $\boldsymbol{S}$.

TABLE I
BOUNDARIES OF PASSIVITY VIOLATIONS

Imaginary eigenvalues of $\boldsymbol{M}$	Square-root of negative eigenvalues of $\boldsymbol{P}$
1.9851e-013 +8.1067e+001i	0 +8.1067e+001i
1.9851e-013 -8.1067e+001i	0 +8.1070e+001i
5.8556e-013 +8.1070e+001i	0 +8.4079e+001i
5.8556e-013 -8.1070e+001i	0 +8.4557e+001i
-5.8265e-013 +8.4079e+001i	0 +8.4786e+001i
-5.8265e-013 -8.4079e+001i	0 +8.5196e+001i
-2.0210e-012 +8.4557e+001i	0 +8.7327e+001i
-2.0210e-012 -8.4557e+001i	0 +8.7369e+001i
4.4409e-013 +8.4786e+001i	
4.4409e-013 -8.4786e+001i	
4.0867e-013 +8.5196e+001i	
4.0867e-013 -8.5196e+001i	
-7.8160e-014 +8.7327e+001i	
-7.8160e-014 -8.7327e+001i	
-2.1991e-012 +8.7369e+001i	
-2.1991e-012 -8.7369e+001i	

the right column are exactly zero. The computation with $\boldsymbol{M}$ and $\boldsymbol{P}$ was 3.0 and 0.64 ms, respectively.

Fig. 3 shows the singular values of $\boldsymbol{S}$. The crossover frequencies as defined by the square root of the negative real eigenvalues of $\boldsymbol{P}$ are included in the plot with red dots. Clearly, the eigenvalues correctly identify the frequencies where the singular values are unity.

VIII. EXAMPLE: PACKAGE APPLICATION

This example considers the S-parameter modeling of a surface mount package [9]. The example has 28 ports. Using vector fitting, a symmetrical pole-residue model is obtained with 40 pole-residue terms and a constant term ($\boldsymbol{D}$), which is converted into a real-only state-space model by (20). The singular values of $\boldsymbol{S}$ are shown in Fig. 4.

Table II compares the CPU time needed for computing the eigenvalues of $\boldsymbol{M}$ and $\boldsymbol{P}$, respectively. It is seen that the usage of $\boldsymbol{P}$ reduces the computation time by a factor 7.4, which is close to the theoretical value of eight. ($\boldsymbol{P}$ was computed from $\boldsymbol{A}$, $\boldsymbol{B}$, $\boldsymbol{C}$, and $\boldsymbol{D}$ by (18) in 3.3 s).

Figs. 5 and 6 show the singular values of $\boldsymbol{S}$ at low and high frequencies, respectively. It is seen that the square roots of the negative eigenvalues of $\boldsymbol{P}$ (indicated by dots) correctly identify the crossover frequencies.

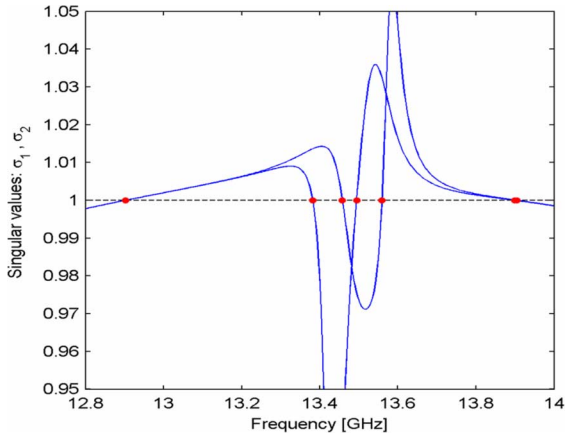

Fig. 3. Singular values of $\boldsymbol{S}$ and crossover frequencies calculated via $\boldsymbol{P}$.

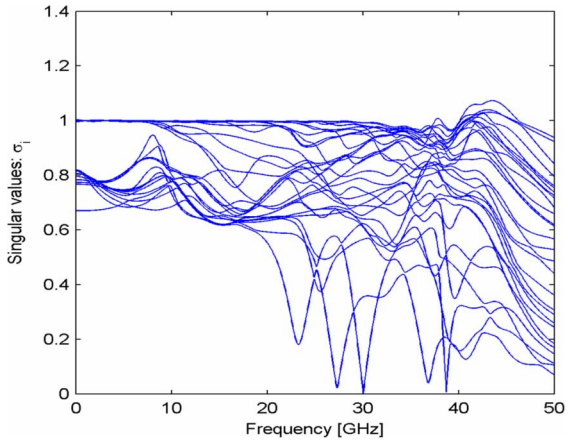

Fig. 4. Rational model: singular values of $\boldsymbol{S}$.

TABLE II
TIME CONSUMPTION FOR EIGENVALUE COMPUTATION

Matrix	Size	CPU time for diagonalization [s]
$\boldsymbol{M}$	2240	109.4
$\boldsymbol{P}$	1120	14.7

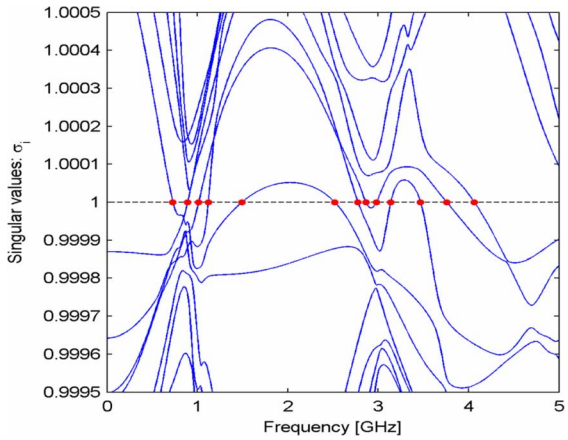

Fig. 5. Singular values of $\boldsymbol{S}$ and crossover frequencies calculated via $\boldsymbol{P}$. Low frequencies.

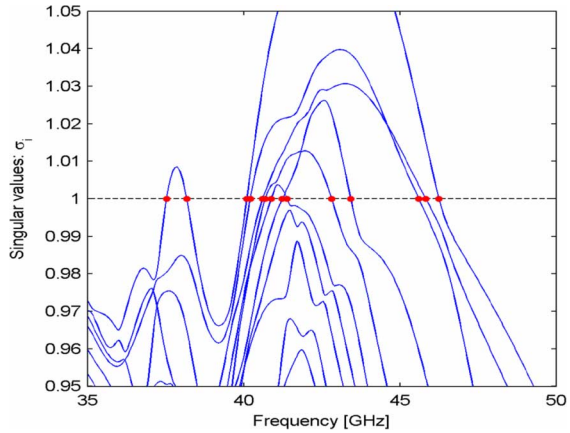

Fig. 6. Singular values of $\boldsymbol{S}$ and crossover frequencies calculated via $\boldsymbol{P}$. High frequencies.

$$\boldsymbol{R}_1 = \begin{bmatrix} 0.3 & 0.1 \\ 0.1 & 0.4 \end{bmatrix}, \boldsymbol{R}_{2,3} = \begin{bmatrix} 4 \pm j5 & 2 \pm j3 \\ 2 \pm j3 & 3 \pm j4 \end{bmatrix}, \boldsymbol{D} = \begin{bmatrix} 0.2 & 0.1 \\ 0.1 & 0.3 \end{bmatrix}$$

$$a_1 = -1, a_{2,3} = -5 \pm j6$$

Fig. 7. Parameters of pole-residue model.

$$\boldsymbol{A} = \left[\begin{array}{ccc|ccc} -1 & 0 & 0 & 0 & 0 & 0 \\ 0 & -5 & 6 & 0 & 0 & 0 \\ 0 & -6 & -5 & 0 & 0 & 0 \\ \hline 0 & 0 & 0 & -1 & 0 & 0 \\ 0 & 0 & 0 & 0 & -5 & 6 \\ 0 & 0 & 0 & 0 & -6 & -5 \end{array}\right], \boldsymbol{B} = \left[\begin{array}{c|c} 1 & 0 \\ 2 & 0 \\ 0 & 0 \\ \hline 0 & 1 \\ 0 & 2 \\ 0 & 0 \end{array}\right]$$

$$\boldsymbol{C} = \left[\begin{array}{ccc|ccc} 0.3 & 4 & 5 & 0.1 & 2 & 3 \\ \hline 0.1 & 2 & 3 & 0.4 & 3 & 4 \end{array}\right], \boldsymbol{D} = \left[\begin{array}{c|c} 0.2 & 0.1 \\ \hline 0.1 & 0.3 \end{array}\right]$$

Fig. 8. Parameters of real-only state-space model.

```
-2.2979 -110.2170  -55.8182   -2.7337  -72.0235  -45.9883
-4.6346 -205.6276 -139.6364   -5.0029 -132.1760  -73.9120
 2.9419   98.7097   37.0000    0.6968   17.8065   27.0968
-2.5578  -85.6070  -52.5455   -2.7795  -92.7683  -46.6158
-4.6510 -160.8915  -89.0909   -5.1331 -178.9883 -130.0059
 0.6968   15.4839   24.0000    3.6387   86.3226   23.8387
```

Fig. 9. Elements of passivity matrix, $\boldsymbol{P}$.

IX. Example: Synthetic Model

Here, we demonstrate the complete passivity test procedure for a synthetic example so that the reader can verify his own computations. The example is a two-port scattering matrix defined by a third-order pole-residue model (1). The parameters of the model are listed in Fig. 7.

Fig. 8 shows the parameters of the corresponding real-only state-space model, obtained via (4), the procedure in Appendix A, and (20).

Fig. 9 shows the elements of the passivity matrix $\boldsymbol{P}$. This matrix is calculated from the state-space model using (18).

Table III shows that the square root of the eigenvalues of $\boldsymbol{P}$ (left column) are equal to the eigenvalues of $\boldsymbol{M}$ (8) (right column), but without redundant information. The purely imaginary elements (contained in dashed boxes) identify the frequencies $(j\omega)$ where the singular values become unity. This result is verified in Fig. 10: the singular values cross the unity line at frequencies 4.24 and 16.43 rad/s.

TABLE III
Square Root of Eigenvalues of $\boldsymbol{P}$. Eigenvalues of $\boldsymbol{M}$

Square-root of eigenvalues of $\boldsymbol{P}$	Eigenvalues of $\boldsymbol{M}$
0 +1.6434e+001i	-8.8818e-016 +1.6434e+001i
4.5242e+000 +6.4558e+000i	-8.8818e-016 -1.6434e+001i
4.5242e+000 -6.4558e+000i	-4.5242e+000 +6.4558e+000i
0 +4.2472e+000i	-4.5242e+000 -6.4558e+000i
9.5267e-001	4.5242e+000 +6.4558e+000i
8.7391e-001	4.5242e+000 -6.4558e+000i
	2.3870e-015 +4.2472e+000i
	2.3870e-015 -4.2472e+000i
	-9.5267e-001
	-8.7391e-001
	9.5267e-001
	8.7391e-001

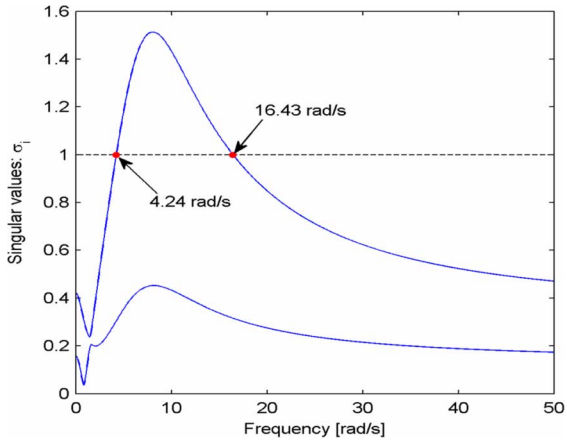

Fig. 10. Singular values of $\boldsymbol{S}$ and crossover frequencies calculated via $\boldsymbol{P}$.

X. Discussion

The half-size test matrix $\boldsymbol{P}$ [see (18)] is valid provided that the state-space model represents a symmetrical $\boldsymbol{S}$. This type of model can easily be obtained by subjecting the upper triangle of $\boldsymbol{S}$ to vector fitting. The simultaneous fitting of many matrix elements can be time consuming, which has formerly motivated the use of columnwise fitting [16], leading to a private pole set for each matrix column. This gives an unsymmetrical state-space model, and thus the half-size test matrix cannot be used. However, the recent introduction of a fast implementation of vector fitting [17] has solved much of the speed issue. For instance, each vector fitting iteration (fast implementation) required only about 7 s for the package example in Section VIII with 201 frequency samples. Therefore, the use of pole-residue modeling is applicable also to large cases.

Application of $\boldsymbol{P}$ also requires that the matrices $(\boldsymbol{D}+\boldsymbol{I})$ and $(\boldsymbol{D}-\boldsymbol{I})$ are nonsingular, in order to facilitate the matrix inversions in (18). Limitations on $\boldsymbol{D}$ also exist with $\boldsymbol{M}$; see (8).

XI. Conclusion

A new test matrix $\boldsymbol{P}$ has been introduced for the passivity assessment of S-parameter based rational models.

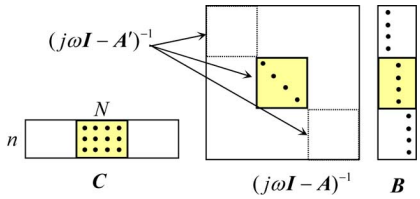

Fig. 11. Columnwise realization of (4).

1) The square root of its negative-real eigenvalues define the frequencies where the singular values of $\boldsymbol{S}$ cross the bound of unity, i.e., the borders of passivity violations.
2) The new passivity test matrix $\boldsymbol{P}$ is only of half the size of the Hamiltonian matrix which has been traditionally used for passivity assessment. Usage of the new test matrix gives a reduction in the time needed for the eigenvalue computation by a factor of nearly eight.
3) The applicability of the new test matrix is restricted to symmetrical state-space models. Such models are obtained by fitting a (symmetrical) pole-residue model to $\boldsymbol{S}$.

Appendix A
Columnwise Realization of State-Space Model

The state-space model (4) is converted into a columnwise realization by interchanging columns in $\boldsymbol{C}$, rows in $\boldsymbol{B}$, and rows and columns in $\boldsymbol{A}$. The resulting structure is illustrated in Fig. 11 for the previous example in Fig. 1 ($n = 3, N = 4$). $\boldsymbol{A}$ gets a submatrix $\boldsymbol{A}'$ of dimension N (with distinct poles) which is repeated n times on the diagonal, and $\boldsymbol{B}$ gets n columns of ones. The ith partition of $\boldsymbol{C}$ contains the concatenation of the ith column of the N residue matrices. It is noted that each column of $\boldsymbol{S}$ is in effect represented by a separate block in $\boldsymbol{C}$ and in $\boldsymbol{A}$. Complex pairs appear in consecutive entries on the diagonal of $\boldsymbol{A}$ (and columns of $\boldsymbol{C}$).

Appendix B
Derivation of Hamiltonian Matrix

For the transfer function $\boldsymbol{y} = \boldsymbol{H}\boldsymbol{u}$, we require with a unit input $\boldsymbol{u}$ that the output be bounded by unity

$$\boldsymbol{y}^H\boldsymbol{y} < 1. \tag{21}$$

The Hamiltonian is defined by the condition that the inequality (21) becomes equality, which is a singularity requirement for loss of passivity. For this, we write

$$\boldsymbol{u}^H\boldsymbol{H}^H\boldsymbol{H}\boldsymbol{u} - 1 = \boldsymbol{u}^H(\boldsymbol{H}^H\boldsymbol{H} - \boldsymbol{I})\boldsymbol{u} = 0. \tag{22}$$

This leads us, with $|\boldsymbol{u}| \neq 0$, to find when

$$\boldsymbol{w} = (\boldsymbol{H}^H\boldsymbol{H} - \boldsymbol{I})\boldsymbol{u} = 0. \tag{23}$$

From (23), we see that $\boldsymbol{u}$ first acts on $\boldsymbol{H}$ (with state-space parameters $\boldsymbol{A}$, $\boldsymbol{B}$, $\boldsymbol{C}$, and $\boldsymbol{D}$). Then, the output $\boldsymbol{y}_1$ becomes the input to $\boldsymbol{H}^H$ (with the respective state-space parameters $\boldsymbol{A}^H$, $\boldsymbol{C}^H$, $\boldsymbol{B}^H$, and $\boldsymbol{D}^H$). From the output $\boldsymbol{y}_2$ of the latter model, we subtract $\boldsymbol{u}$ itself. This gives

$$j\omega\boldsymbol{x}_1 = \boldsymbol{A}\boldsymbol{x}_1 + \boldsymbol{B}\boldsymbol{u} \tag{24a}$$
$$\boldsymbol{y}_1 = \boldsymbol{C}\boldsymbol{x}_1 + \boldsymbol{D}\boldsymbol{u} \tag{24b}$$
$$-j\omega\boldsymbol{x}_2 = \boldsymbol{A}^H\boldsymbol{x}_2 + \boldsymbol{C}^H\boldsymbol{y}_1 \tag{25a}$$
$$\boldsymbol{y}_2 = \boldsymbol{B}^H\boldsymbol{x}_2 + \boldsymbol{D}^H\boldsymbol{y}_1 \tag{25b}$$
$$\boldsymbol{w} = \boldsymbol{y}_2 - \boldsymbol{u} = 0. \tag{25c}$$

If we substitute $\boldsymbol{y}_1$ from (24b) into (25a) and (25b) and $\boldsymbol{y}_2$ from (25b) into (25c), the above equations become

$$j\omega\boldsymbol{x}_1 = \boldsymbol{A}\boldsymbol{x}_1 + \boldsymbol{B}\boldsymbol{u} \tag{26a}$$
$$j\omega\boldsymbol{x}_2 = -\boldsymbol{A}^H\boldsymbol{x}_2 - \boldsymbol{C}^H(\boldsymbol{C}\boldsymbol{x}_1 + \boldsymbol{D}\boldsymbol{u}) \tag{26b}$$
$$\boldsymbol{w} = \boldsymbol{B}^H\boldsymbol{x}_2 + \boldsymbol{D}^H(\boldsymbol{C}\boldsymbol{x}_1 + \boldsymbol{D}\boldsymbol{u}) - \boldsymbol{u} = 0 \tag{26c}$$

or

$$j\omega\begin{bmatrix}\boldsymbol{x}_1\\ \boldsymbol{x}_2\end{bmatrix} = \begin{bmatrix}\boldsymbol{A} & 0\\ -\boldsymbol{C}^H\boldsymbol{C} & -\boldsymbol{A}^H\end{bmatrix}\begin{bmatrix}\boldsymbol{x}_1\\ \boldsymbol{x}_2\end{bmatrix} + \begin{bmatrix}\boldsymbol{B}\\ -\boldsymbol{C}^H\boldsymbol{D}\end{bmatrix}\boldsymbol{u} \tag{27a}$$

$$\boldsymbol{w} = \begin{bmatrix}\boldsymbol{D}^H\boldsymbol{C} & \boldsymbol{B}^H\end{bmatrix}\begin{bmatrix}\boldsymbol{x}_1\\ \boldsymbol{x}_2\end{bmatrix} + (\boldsymbol{D}^H\boldsymbol{D} - \boldsymbol{I})\boldsymbol{u}. \tag{27b}$$

From (27b), we substitute $\boldsymbol{u}$ into (27a) and get

$$j\omega\begin{bmatrix}\boldsymbol{x}_1\\ \boldsymbol{x}_2\end{bmatrix} = \left(\begin{bmatrix}\boldsymbol{A} & 0\\ -\boldsymbol{C}^H\boldsymbol{C} & -\boldsymbol{A}^H\end{bmatrix} - \boldsymbol{K}\right)\begin{bmatrix}\boldsymbol{x}_1\\ \boldsymbol{x}_2\end{bmatrix} \tag{28}$$

where

$$\boldsymbol{K} = \begin{bmatrix}\boldsymbol{B}\\ -\boldsymbol{C}^H\boldsymbol{D}\end{bmatrix}(\boldsymbol{D}^H\boldsymbol{D} - \boldsymbol{I})^{-1}\begin{bmatrix}\boldsymbol{D}^H\boldsymbol{C} & \boldsymbol{B}^H\end{bmatrix}. \tag{29}$$

This can be rewritten as

$$j\omega\begin{bmatrix}\boldsymbol{x}_1\\ \boldsymbol{x}_2\end{bmatrix} = \begin{bmatrix}\boldsymbol{A} - \boldsymbol{B}\hat{\boldsymbol{R}}^{-1}\boldsymbol{D}^H\boldsymbol{C} & -\boldsymbol{B}\hat{\boldsymbol{R}}^{-1}\boldsymbol{B}^H\\ \boldsymbol{C}^H\hat{\boldsymbol{S}}^{-1}\boldsymbol{C} & -\boldsymbol{A}^H + \boldsymbol{C}^H\boldsymbol{D}\hat{\boldsymbol{R}}^{-1}\boldsymbol{B}^H\end{bmatrix}\begin{bmatrix}\boldsymbol{x}_1\\ \boldsymbol{x}_2\end{bmatrix} \tag{30}$$

where

$$\hat{\boldsymbol{R}} = \boldsymbol{D}^H\boldsymbol{D} - \boldsymbol{I} \tag{31a}$$
$$\hat{\boldsymbol{S}} = \boldsymbol{D}\boldsymbol{D}^H - \boldsymbol{I}. \tag{31b}$$

Thus, the Hamiltonian matrix is

$$\boldsymbol{M} = \begin{bmatrix} \boldsymbol{A} - \boldsymbol{B}\hat{\boldsymbol{R}}^{-1}\boldsymbol{D}^H\boldsymbol{C} & -\boldsymbol{B}\hat{\boldsymbol{R}}^{-1}\boldsymbol{B}^H \\ \boldsymbol{C}^H\hat{\boldsymbol{S}}^{-1}\boldsymbol{C} & -\boldsymbol{A}^H + \boldsymbol{C}^H\boldsymbol{D}\hat{\boldsymbol{R}}^{-1}\boldsymbol{B}^H \end{bmatrix} \quad (32)$$

and its imaginary eigenvalues $j\omega$ [as shown in (30)] give the frequencies ω for which (23) is satisfied and the matrix $\boldsymbol{H}^H\boldsymbol{H} - \boldsymbol{I}$ is singular.

Since the model is assumed to satisfy the conjugacy property $\boldsymbol{H}(j\omega) = \boldsymbol{H}^*(-j\omega)$, where the asterisk denotes conjugate, the transfer function $\boldsymbol{H}(j\omega)$ does not change if the state-space matrices $\boldsymbol{A}$, $\boldsymbol{C}$, $\boldsymbol{B}$, $\boldsymbol{D}$ are replaced with their conjugate counterparts. Thus, the Hermitian transpose in (32) can be replaced with simple transpose and (32) becomes equal to (8).

Appendix C
Conversion Into a Real State-Space Model

The state-space model in complex form can be written as

$$\begin{bmatrix} \dot{\boldsymbol{x}}_1 \\ \dot{\boldsymbol{x}}_2 \\ \dot{\boldsymbol{x}}_3 \end{bmatrix} = \begin{bmatrix} \boldsymbol{A}_r & 0 & 0 \\ 0 & \boldsymbol{A}_c & 0 \\ 0 & 0 & \boldsymbol{A}_c^* \end{bmatrix} \begin{bmatrix} \boldsymbol{x}_1 \\ \boldsymbol{x}_2 \\ \boldsymbol{x}_3 \end{bmatrix} + \begin{bmatrix} \boldsymbol{B}_r \\ \boldsymbol{B}_c \\ \boldsymbol{B}_c^* \end{bmatrix} \boldsymbol{u} \quad (33a)$$

$$\boldsymbol{y} = [\boldsymbol{C}_r \quad \boldsymbol{C}_c \quad \boldsymbol{C}_c^*] \begin{bmatrix} \boldsymbol{x}_1 \\ \boldsymbol{x}_2 \\ \boldsymbol{x}_3 \end{bmatrix} + \boldsymbol{D}\boldsymbol{u} \quad (33b)$$

where the transition matrix $\boldsymbol{A}$ is diagonal. Subscripts r and c denote the partitions with real and complex poles, respectively.

Introducing the similarity transformation [14]

$$\tilde{\boldsymbol{x}} = \boldsymbol{T}^{-1}\boldsymbol{x} \quad (34)$$

where

$$\boldsymbol{T}^{-1} = \begin{bmatrix} \boldsymbol{I} & 0 & 0 \\ 0 & \boldsymbol{I} & \boldsymbol{I} \\ 0 & j\boldsymbol{I} & -j\boldsymbol{I} \end{bmatrix} \quad (35)$$

gives a new state-space model with real matrices

$$\tilde{\boldsymbol{A}} = \boldsymbol{T}^{-1}\boldsymbol{A}\boldsymbol{T} = \begin{bmatrix} \boldsymbol{A}_r & 0 & 0 \\ 0 & \mathrm{Re}\{\boldsymbol{A}_c\} & \mathrm{Im}\{\boldsymbol{A}_c\} \\ 0 & -\mathrm{Im}\{\boldsymbol{A}_c\} & \mathrm{Re}\{\boldsymbol{A}_c\} \end{bmatrix} \quad (36a)$$

$$\tilde{\boldsymbol{B}} = \boldsymbol{T}^{-1}\boldsymbol{B} = \begin{bmatrix} \boldsymbol{B}_r \\ 2\mathrm{Re}\{\boldsymbol{B}_c\} \\ -2\mathrm{Im}\{\boldsymbol{B}_c\} \end{bmatrix} \quad (36b)$$

$$\tilde{\boldsymbol{C}} = \boldsymbol{C}\boldsymbol{T} = [\boldsymbol{C}_r \quad \mathrm{Re}\{\boldsymbol{C}_c\} \quad \mathrm{Im}\{\boldsymbol{C}_c\}]$$

$$\tilde{\boldsymbol{D}} = \boldsymbol{D}. \quad (36c)$$

In the following, we show that the transformation (34) will not change the eigenvalues of the passivity matrix $\boldsymbol{P}$ [(18)].

Introducing the transformation (36a)–(36c) into (18), we obtain

$$\boldsymbol{P} = (\boldsymbol{T}\tilde{\boldsymbol{A}}\boldsymbol{T}^{-1} - \boldsymbol{T}\tilde{\boldsymbol{B}}(\tilde{\boldsymbol{D}} - \boldsymbol{I})^{-1}\tilde{\boldsymbol{C}}\boldsymbol{T}^{-1}) \cdot (\boldsymbol{T}\tilde{\boldsymbol{A}}\boldsymbol{T}^{-1} - \boldsymbol{T}\tilde{\boldsymbol{B}}(\tilde{\boldsymbol{D}} + \boldsymbol{I})^{-1}\tilde{\boldsymbol{C}}\boldsymbol{T}^{-1}) \quad (37)$$

or, after some simplifications, we have

$$\boldsymbol{P} = \boldsymbol{T}(\tilde{\boldsymbol{A}} - \tilde{\boldsymbol{B}}(\tilde{\boldsymbol{D}} - \boldsymbol{I})^{-1}\tilde{\boldsymbol{C}})(\tilde{\boldsymbol{A}} - \tilde{\boldsymbol{B}}(\tilde{\boldsymbol{D}} + \boldsymbol{I})^{-1}\tilde{\boldsymbol{C}})\boldsymbol{T}^{-1}. \quad (38)$$

We thus have

$$\boldsymbol{P} = \boldsymbol{T}\tilde{\boldsymbol{P}}\boldsymbol{T}^{-1}. \quad (39)$$

This shows that the eigenvalues of $\boldsymbol{P}$ can be obtained as those of $\tilde{\boldsymbol{P}}$ since the two are related by the similarity transformation (39). Thus, instead of (19), we use the equation

$$\lambda_{\boldsymbol{M}} = \pm\sqrt{\tilde{\lambda}_{\boldsymbol{P}}}. \quad (40)$$

Acknowledgment

The authors would like to thank A. Lamecki (Gdansk University of Technology, Gdansk, Poland) for providing the microwave filter example in Section VII and Prof. S. Grivet-Talocia (Politecnico di Torino, Turin, Italy) for providing the package example in Section VIII.

References

[1] B. Gustavsen and A. Semlyen, "Rational approximation of frequency domain responses by vector fitting," *IEEE Trans. Power Del.*, vol. 14, no. 3, pp. 1052–1061, Jul. 1999.

[2] B. Gustavsen, "Improving the pole relocating properties of vector fitting," *IEEE Trans. Power Del.*, vol. 21, no. 3, pp. 1587–1592, Jul. 2006.

[3] D. Deschrijver, B. Haegeman, and T. Dhaene, "Orthonormal vector fitting: A robust macromodeling tool for rational approximation of frequency domain responses," *IEEE Trans. Adv. Packag.*, vol. 30, no. 2, pp. 216–225, May 2007.

[4] B. Gustavsen and C. Heitz, "Model vector fitting: A tool for generating ration models of high accuracy with arbitrary terminal conditions," *IEEE Trans. Adv. Packag.*, to be published.

[5] S. Grivet-Talocia, "Package macromodeling via time-domain vector fitting," *IEEE Microw. Wireless Compon. Lett.*, vol. 13, no. 11, pp. 472–474, Nov. 2003.

[6] Y. S. Mekonnen and J. E. Schutt-Ainé, "Broadband macromodeling of sampled frequency data using z-domain vector-fitting method," in *Proc. 11th IEEE Workshop Signal Propag. on Interconnects*, Ruta di Camogli (Genova), Italy, May 13–16, 2007, pp. 45–48.

[7] S. Boyd, V. Balakrishnan, and P. Kabamba, "A bisection method for computing H_∞ norm of a transfer matrix and related problems," *Math. Control Signals Syst.*, vol. 2, pp. 207–219, 1989.

[8] D. Saraswat, R. Achar, and M. S. Nakhla, "A fast algorithm and practical considerations for passive macromodeling of measured/simulated data," *IEEE Trans. Adv. Packag.*, vol. 27, no. 1, pp. 57–70, Feb. 2004.

[9] S. Grivet-Talocia, "Passivity enforcement via perturbation of Hamiltonian matrices," *IEEE Trans. Circuits Syst. I, Reg. Papers*, vol. 51, no. 9, pp. 1755–1769, Sep. 2004.

[10] S. Grivet-Talocia, "Fast passivity enforcement for large and sparse macromodels," in *Proc. 13th IEEE Top. Meeting Elect. Performance Electron. Packag.*, Portland, OR, Oct. 25–27, 2004, pp. 247–250.

[11] S. Grivet-Talocia, "An adaptive sampling technique for passivity characterization and enforcement of large interconnect macromodels," *IEEE Trans. Adv. Packag.*, vol. 30, no. 2, pp. 226–237, May 2007.
[12] A. Semlyen and B. Gustavsen, "A half-size singularity test matrix for fast and reliable passivity assessment of rational models," *IEEE Trans. Power Del.*, to be published.
[13] B. Gustavsen and A. Semlyen, "A robust approach for system identification in the frequency domain," *IEEE Trans. Power Del.*, vol. 19, no. 3, pp. 1167–1173, Jul. 2004.
[14] E.-P. Li, E.-X. Liu, L. W. Li, and M.-S. Leong, "A coupled efficient and systematic full-wave time-domain macromodeling and circuit simulation method for signal integrity analysis of high-speed interconnects," *IEEE Trans. Adv. Packag.*, vol. 27, no. 1, pp. 213–223, Feb. 2004.
[15] A. Lamecki and M. Mrozowski, "Equivalent SPICE circuits with guaranteed passivity from nonpassive models," *IEEE Trans. Microw. Theory Tech.*, vol. 55, no. 3, pp. 526–32, Mar. 2007.
[16] B. Gustavsen and A. Semlyen, "Combined phase and modal domain calculation of transmission line transients based on vector fitting," *IEEE Trans. Power Del.*, vol. 13, no. 2, pp. 596–604, Apr. 1998.
[17] D. Deschrijver, M. Mrozowski, T. Dhaene, and D. D. Zutter, "Macromodeling of multiport systems using a fast implementation of the vector fitting method," *IEEE Microw. Wireless Compon. Lett.*, vol. 18, no. 6, pp. 383–385, Jun. 2008.

Bjørn Gustavsen (M'94–SM'03) was born in Harstad, Norway, in 1965. He received the M.Sc. and Dr.Ing. degrees from the Norwegian Institute of Technology (NTH), Trondheim, Norway, in 1989 and 1993, respectively.

Since 1994, he has been with SINTEF Energy Research, Trondheim, Norway. His interests include simulation of electromagnetic transients and modeling of frequency dependent effects. He spent 1996 as a Visiting Researcher with the University of Toronto, Toronto, ON, Canada, and the summer of 1998 with the Manitoba HVDC Research Centre, Winnipeg, MB, Canada. He was a Marie Curie Fellow with the University of Stuttgart, Stuttgart, Germany, from August 2001 to August 2002.

Adam Semlyen (LF'97) was born in Romania in 1923. He received the Dipl. Ing. and Ph.D. degrees.

He began his career in Romania with an electric power utility and held academic positions with the Polytechnic Institute of Timisoara. In 1969, he joined the University of Toronto, Toronto, ON, Canada, where he is a Professor with the Department of Electrical and Computer Engineering, Emeritus since 1988. His research interests include steady-state and dynamic analysis as well as computation of electromagnetic transients in power systems.